MAUSAM, **62**, 3 (July 2011), 441-448

551.521 : 551.510.421

Variation of aerosol optical thickness with atmospheric water vapour : A case study over a continental station Mysore, India

K. E. GANESH, T. K. UMESH* and B. NARASIMHAMURTHY*

PES Institute of Technology, Department of S&H, Bengaluru, India

**Department of Studies in Physics, University of Mysore, Mysore, India*

(*Received 31 March 2010, Modified 8 October 2010*)

e mail : ganeshke@gmail.com; drganeshke@gmail.com

सार – दिसम्बर 2003 से जून 2006 की अवधि के दौरान महाद्वीपीय निम्न अक्षांश वाले स्टेशन मैसूर (12.3 डिग्री उ.) में वायुमंडलीय परिमाप लिए गए। सौर वर्णक्रम के दृश्य और नियर इनफ्रारेड रेंज में 5 पटिट्यों वाले सन फोटोमीटर का उपयोग करते हुए माप लिए गए हैं। वायुमंडलीय जलवाष्प पर एरोसोल ऑप्टीकल थिक्नेस (ए. ओ. टी.) के तरंग दैर्ध्य (वेवलेन्थ) की निर्भरता स्पष्ट करने के लिए विशेष प्रकार के दो वेवलेन्थ चैनल्स प्रयोग किए गए हैं, इनमें एक 500 एन. एम. पर दूसरा 1020 एन. एम. पर है। मौसम विज्ञान की भाषा में शान्त दिनों में ए. ओ. टी. और जल वाष्प के बीच एक रैखिक निर्भरता का देखा जाना एक महत्वपूर्ण प्रेक्षण रहा है। ए. ओ. टी. का विकास दर लम्बे वेवलेन्थ (1020 एन. एम.) के वनिस्पत छोटे वेवलेन्थ (500 एन. एम.) में अधिक पाया गया है। मासिक आधार पर बड़े पैमाने पर एक आलेख तैयार किया गया है वस्तुत यह ए. ओ. टी. और जल वाष्प का एक रेखा चित्र है जो उस माह के साफ आकाश वाले दिनों में लिए गए चित्रों पर आधारित है आगें के परीक्षणो से पता चला है कि कुछ महीनों में जलवाष्प के साथ ए. ओ. टी. की वृद्धि में इकहरी प्रवृति देखी गई है जबकि अन्य महीनों में दोहरी प्रवृति की स्थिति देखी गई है। इन परिणामों से वर्षणीय जलवाष्प युक्त वायुमंडलीय एरोसोल के लक्षणों में हुए परिवर्तनों के बारे में जानकारी प्राप्त हुई है जो इस शोध पत्र की विषय वस्तु है।

ABSTRACT. Atmospheric measurements in a continental, low latitude station Mysore (12.3° N) has been carried out, for the period December 2003 to June 2006. Measurements were made using a sunphotometer with five bands in the visible and near-infrared range of the solar spectrum. To bring out the wavelength dependence of Aerosol Optical Thickness (AOT) on atmospheric water vapour, typically two wavelength channels are being used, one at 500 nm and the other at 1020 nm. A linear dependence between AOT and water vapour on meteorologically calm days is the important observation made. Growth rate of AOT is found to be larger at shorter wavelength (500 nm) than that of the longer wavelength (1020 nm). A mass-plot representation is followed on monthly basis, which is nothing but the graphical plot of spectral AOT versus water vapour of the scans for all the clear sky days of a particular month. Further investigations reveal that some months exhibit a single trend of growth of AOT with water vapour whereas double trend is the scenario for other months. These results provide insight into the changes in the atmospheric aerosol characteristics with precipitable water vapour, which is the subject matter of this paper.

Key words – Atmospheric aerosols, Atmospheric water vapour, AOT, Sunphotometer.

1. Introduction

Water vapour is one of the major variable gaseous constituents of the Earth's atmosphere. As a green house gas, it influences significantly the Earth's radiation budget. Jacob (2001) has discussed the role of water vapour in the atmosphere. Water vapour is constantly added to the atmosphere by evaporation from various water bodies or moist damp ground and by transpiration from plants. Condensation process depletes the atmosphere of water. For these reasons, water vapour content is quite variable. The amount of water vapour present in the atmosphere is expressed by precipitable water. This quantity can be highly variable and shows seasonal variation. An extremely dry atmosphere may contain about 0.1 cm of precipitable water while a humid atmosphere contains about 4 cm (Iqbal, 1983).

Tropospheric aerosols produced by both natural and anthropogenic processes exhibit large temporal and spatial variations (Faizoun *et al*., 1994; Kaufman *et al*., 1994). Depending on the source, the size of aerosol has a range span of $10^{-3} – 10^{2}$ μm. Atmospheric aerosols Mie scatter the solar radiation reaching the ground. The attenuation depends on the number and size of the aerosols. Aerosol Optical Thickness (AOT) quantitatively expresses this

optical phenomenon. Since the solar radiation extends over a range of electromagnetic spectrum, the AOT exhibits a spectral behaviour.

Apart from the climatological importance, water vapour at higher altitudes plays an important role in the growth of aerosol particles (Twomey, 1977). Non-hygroscopic aerosols with the hygroscopic surfaces accumulate a film of water under some conditions. The hygroscopic type acts as centers or nuclei for condensation of water vapour. Because of this potential for particle growth, scattering characteristics change leading to variation in AOT (McCartney, 1976). The location at which measurements were made abounds by greenery with plants and trees. Aromatic hydrocarbon vapours known as terpenes are exuded by foliage. Under the influence of sunlight and ozone, the terpenes nucleate into hygroscopic aerosols.

Prompted by the necessity for understanding the atmospheric aerosols, in this paper a study is reported on the variation of AOT with atmospheric water vapour. The data on AOT and water vapour are obtained with a hand-held sunphotometer. By analyzing the data, the linkage between AOT and water vapour is arrived. In India, several workers have made similar kind of study: Suresh and Elgar (2005) have reported a linear relationship of AOT with water vapour at the west coast of India. Prabha Nair and Krishna Moorthy (1998) have reported an increasing trend of AOT with water vapour for a coastal station Trivandrum. In addition, there are studies other than in India. Eck *et al*. (2001) results have been reported for aerosols over Maldives and in Persian Gulf by Smirnov *et al*. (2002).

2. Theory

The solar radiation traversing through the terrestrial atmosphere undergoes extinction due to three processes. Rayleigh scattering by air molecules, Mie scattering by aerosols, and molecular absorption. Solar radiation is a composite of monochromatic radiations, each of wavelength λ. The spectral radiation V_λ reaching the ground is related to the extra-terrestrial solar radiation $V_{0\lambda}$ through the Bouguer-Lambert-Beer law

$$V_\lambda = V_{0\lambda}\left(\frac{r_0}{r}\right)^2 \exp(-m\tau_\lambda) \qquad (1)$$

In this equation, r_0 and r are the sun-earth distances, mean and the actual respectively; m is the relative air mass which in terms of solar zenith angle χ becomes m = sec χ ; and the last term τ_λ is the integrated columnar extinction also referred to as total optical depth/thickness. V_λ is being generally measured with a sunphotometer;

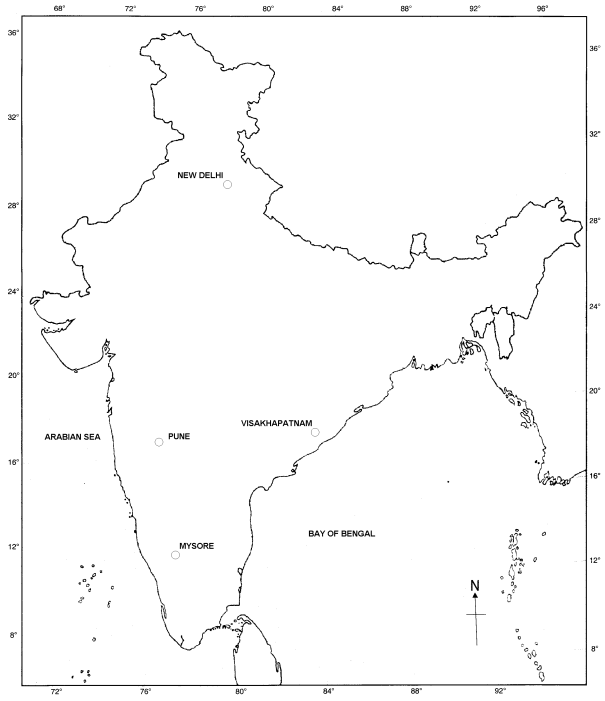

Fig. 1. Geographic identity of Mysore

the output is an electrical signal of voltage *V* volts proportional to the incoming spectral radiation. On a logarithmic scale, the Eqn. (1) is linearised as below:

$$\text{In } V_\lambda = \left[\text{In } V_{0\lambda} + 2\,\text{In}\left(\frac{r_0}{r}\right)\right] - m\tau_\lambda \qquad (2)$$

Graphical representation of this equation is referred to as Langley plot. Zero air mass intercept serves as a calibration constant. The slope gives the total optical depth τ_λ. By subtracting the contributions due to Rayleigh scattering and molecular absorptions from τ_λ AOT is determined. The built-in algorithm in the MICROTOPS II will do all these calculations so quickly. In order to obtain instantaneous value of AOT, the calibration constant is pre determined and linearised with the signal voltage at any instant.

3. Climate of Mysore

Mysore (12° 19′ N and 76° 39′ E), situated at an altitude of 767 m above sea level on the Deccan plateau of peninsular India is a low latitude station with moderate climate. On the East, West and South, about 300-500 km away is the water spreads of Bay of Bengal, Arabian Sea and Indian Ocean respectively (Fig. 1). To the North lies the landmass of Asiatic continent. In any year, the period

June-November, receives monsoon rains, which account for 73% of the average annual rainfall of 760 mm [Narasimhamurthy *et al*., 1998]. Following the rainy season, the winter prevails through December-February. During this season, the temperature is low and the rainfall is about 3%. The hot months March-May constitute the summer and account for 24% rainfall. An overall range of temperature of the year lies between 18-36° C (Ganesh *et al*., 2009).

4. Method of data collection

In order to collect the solar radiation a hand-held multi-band sunphotometer MICROTOPS II developed by Solar Light Company, USA (2002) is used. The instrument is equipped with five accurately aligned optical collimators with a full field view of 2.5°. Internal baffles are also integrated into the device to eliminate internal reflections. Each channel is fitted with a narrow-band interference filter and a photodiode suitable for the particular wavelength range. The MICROTOPS II used in the present study has optical filters transmitting the radiation centered at wavelengths of 440, 500, 675, 936 and 1020 nm. The collimators are encapsulated in a cast aluminum optical block for stability. A sun target and pointing assembly is permanently attached to the optical block and laser-aligned to ensure accurate alignment with the optical channels. When the image of the Sun is centered in the bull's-eye of the Sun target, all optical channels are oriented directly at the solar disk. Radiation captured by the collimator and band pass filters reaches the photodiodes, producing an electrical current that is proportional to the radiant power intercepted by the photodiodes. The current is first amplified and then converted to a digital signal by a high resolution Analog to Digital converter. The signals from the photodiodes are processed in series. However, with 20 conversions per second, the results can be treated as if the photodiodes were read simultaneously. AOT is determined by Langley method assuming the validity of the Bouguer-Lambert-Beer law. The optical depth due to Rayleigh scattering is subtracted from the total optical depth to obtain AOT. The calculation algorithms are programmed in the photometer and the results of all stored scans can be conveniently viewed on the LCD. The raw data are also stored to allow retrospective adjustments of calibration constants.

Initially, several MICROTOPS II settings are made with the help of GPS receiver. These include Universal date and time, geographic coordinates, altitude and atmospheric pressure of the measurement site.

For the observations, the MICROTOPS II is mounted on a tripod in order to minimize the Sun targeting error and is stationed on the open terrace of a two-storey building located in an unpolluted area. On the days of clear sky, *viz*., when there are no clouds, the measurements are made. The data are collected during 0430 - 1100 UTC at fifteen minutes interval.

5. Calibration

The instrument was calibrated at regular intervals. The degradation of the filters or the drift in the calibration values was found to be marginal. The calibration was carried out atop Sri Chamundeshwari Hills, which is at about 300 m from the ground level using the standard Langley technique. The calibration constants obtained from the data collected atop the hill did not show any large variations from the values obtained from the calibrations at factory (Ganesh *et al*., 2009).

6. Estimation of water vapour in the atmosphere

The amount of water vapour present in the atmosphere can be defined in many ways. One of the ways is as follows: the amount of water vapour along a path is defined as the thickness of the liquid water that would be formed if all the vapour in the zenith were condensed at the surface of a unit area. It is expressed either in centimeter or in g cm^{-2}. A height of 1 cm therefore corresponds to 1g cm^{-2} of precipitable water. In literature, both these units are commonly employed.

Water vapor calculation has been made based on the extraterrestrial constant of the 936 nm channel, its signal, time, location, water vapor calibration constants and AOT at 936 nm. Once again, by making use of Bouguer-Lambert-Beer law for the 936 nm channel, which is located in the water vapor absorption band, the water vapor column in centimeter is calculated as follows:

$$W = \left[\frac{\ln(V_{0w}) - \ln(V_w \times \mathrm{SDCORR}) - \tau_{aw} \times M}{K \times M^{B}} \right]^{1/B} \quad (3)$$

where the index "w" refers to the 936 nm water vapor channel, ln (V_{0w}) is the AOT calibration constant, V_w is the signal intensity in milli volts, SDCORR is the mean earth-sun distance correction, M is the optical airmass, τ_{aw} is the aerosol optical thickness and K&B are the water vapor calibration constants dependent on the spectral transmission of the 936 nm channel (Solar Light Company, USA, 2002).

7. Angstrom's turbidity parameters

Atmospheric turbidity depends on both the number and size of aerosols. Angstrom relates these two parameters with the AOT (τ_λ) which has a spectral

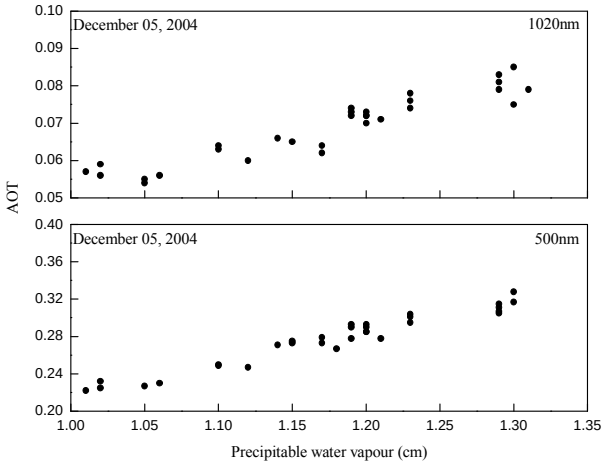

Fig. 2. Plot of AOT versus precipitable water vapour (cm)

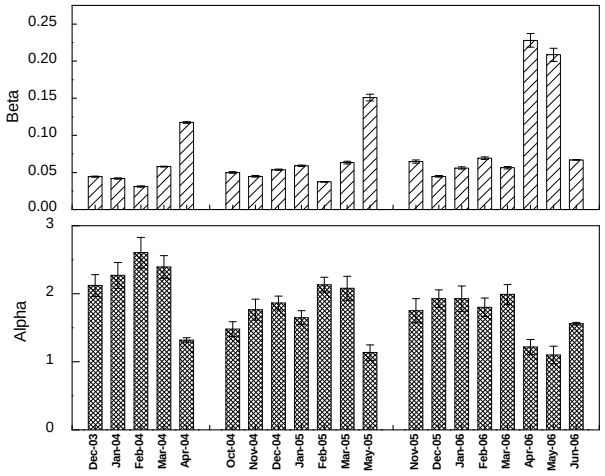

Fig. 3. Monthly averages of α and β

dependence and is a measure of extinction of solar radiation by the aerosols at wavelength λ as

$$\tau_\lambda = \beta\lambda^{-\alpha} \quad (4)$$

In this equation β is called the turbidity coefficient and α the wavelength exponent. Very often Angstrom's method is considered as the best method (Cachorro *et al*., 1987). These are dependent respectively on the number and the size of aerosols. Large values of α indicate a relatively high ratio of small particles to large particles. Further, the wavelength λ is in micrometer (Iqbal, 1983). The Angstrom equation (4) delineates into linear form on logarithmic scale

$$\ln \tau_\lambda = \ln\beta - \alpha\ln\lambda \quad (5)$$

TABLE 1

Slope values for the plots of AOT versus water vapour

Date	Slope	
	500 nm	1020 nm
December 08, 2003	0.28	0.11 ± 0.010
March 05, 2004	0.46	0.13 ± 0.030
December 05, 2004	0.34	0.07 ± 0.009
February 10, 2005	0.21	0.13 ± 0.040
March 18, 2005	0.29	0.08 ± 0.020
April 28, 2005	0.20	0.15 ± 0.020
May 17, 2005	0.13	0.16 ± 0.020
January 12, 2006	0.18	0.06 ± 0.008
February 22, 2006	0.72	0.27 ± 0.060
June 12, 2006	0.16	0.10 ± 0.030

By a logarithmic regression analysis and least squares fit of each of the scans one set of values for α and β is obtained.

8. Results

To bring out the wavelength dependence of AOT on atmospheric water vapour, two wavelengths are considered, one at 500 nm and the other at 1020 nm. Graphical plots of AOT versus water vapour are made for each day of observation. It is found that the AOT and water vapour exhibit a linear dependence on meteorologically calm days (*i.e*., days without large atmospheric perturbations). Fig. 2 is a typical representation of the plot of AOT versus water vapour for two wavelengths. The slope of this graph represents the ratio of change in AOT to that of water vapour and the intercept represents solar extinction other than atmospheric water vapour which is very less. This strengthens the fact that atmospheric water vapour is the supporter for the growth of aerosol particles. For each of the days slope is determined by least-squares method. It is found that the values of slope are higher for shorter wavelength compared to that of longer wavelength. This indicates that growth rate of AOT is larger at shorter wavelength than that of the longer wavelength. Larger growth rate at shorter wavelength is an indication of increase in the number of small sized particles. The Angstrom's parameter α which is a measure of concentration of small sized particles is generally high (Fig. 3). In Table 1 are given the values of slope typically for ten days. The rate of growth as indicated by the slope is observed to be dependent on the range of water vapour over the day.

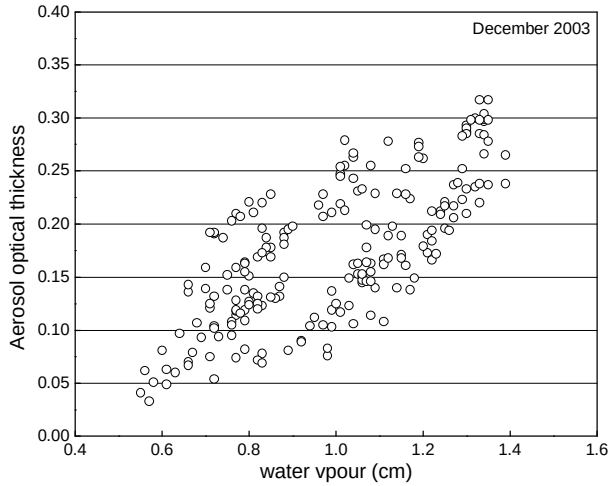

Fig. 4. Single trend behaviour of AOT with water vapour

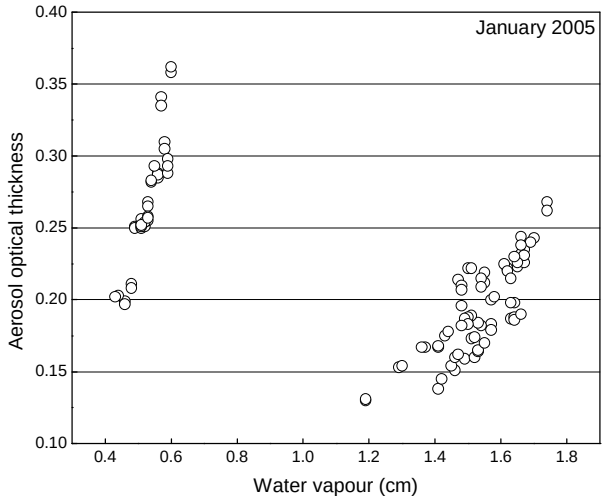

Fig. 5. Double trend behaviour of AOT with water vapour

With the data of 120 days, analysis of the influence of water vapour on AOT on daily basis becomes rather difficult though not impossible. It was therefore considered appropriate to treat the data month-wise. Further, a larger water vapour range is encountered during any month which helps in a better understanding of growth rate of aerosols. For any single month, a mass-plot representation is followed.

Mass-plot is a graphical plot of AOT versus water vapour for a single wavelength of the scans for all the clear sky days of a particular month. This method of approach is followed typically for the wavelengths 500 nm and 1020 nm as described below.

TABLE 2

Slope values for the mass-plot of AOT versus water vapour [@ 500nm] for different months during three years

Month	Slope	Range of water vapour in cm (min – max)
December 2003	0.21	0.55-1.43
January 2004	0.27	0.54-1.06
	0.53	1.06-1.30
February 2004	0.22	0.53-0.98
March 2004	0.19	0.50-1.81
April 2004	0.12	1.54-2.59
December 2004	0.22	0.41-1.31
	0.12	0.91-1.83
January 2005	0.22	1.18-1.73
	0.84	0.42-0.60
February 2005	0.22	0.60-1.46
	0.42	0.46-0.75
March 2005	0.23	0.73-1.81
November 2005	0.23	0.90-1.82
	0.42	0.74-1.02
December 2005	0.13	1.05-2.12
	0.46	0.52-0.84
January 2006	0.31	0.50-1.43
	0.26	1.63-2.52
February 2006	0.21	0.44-1.37
	0.37	1.11-1.94
March 2006	0.26	1.80-2.60
	0.3	1.10-2.00
April 2006	0.29	1.57-2.39
May 2006	0.39	2.13-2.39
	0.31	2.07-2.51
June 2006	0.16	2.29-2.49

8.1. *Growth rate features of AOT at 500 nm*

Starting with the month December 2003, for each month the AOTs and the corresponding water vapour are

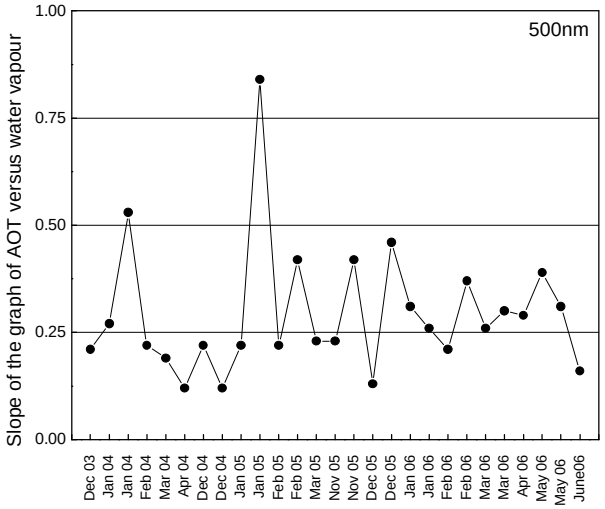

Fig. 6. Slope of the graph of AOT versus water vapour over different months at 500nm

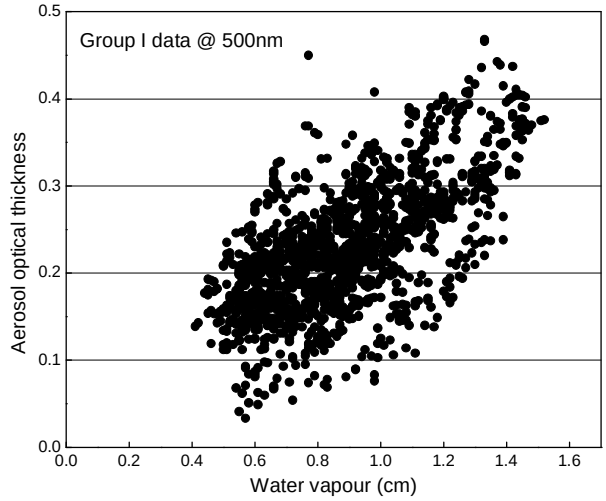

Fig. 7. Mass plot of AOT versus water vapour for Group I data sets at 500 nm

plotted for 500 nm producing a mass plot graphical representation. On examining the mass-plots, a linear variation of AOT with water vapour is observed. It was further noticeable that some months exhibit a single trend of growth of AOT with water vapour, whereas in some months there were two trends. Of the two trends, one gave a larger slope for low water vapour content, whereas the other one gave a smaller slope when the water vapour content is high. Figs. 4&5 are the typical representations of the single and double trends respectively. Table 2 presents the values of slopes with 5-10% error, together with the range of water vapour for the months of

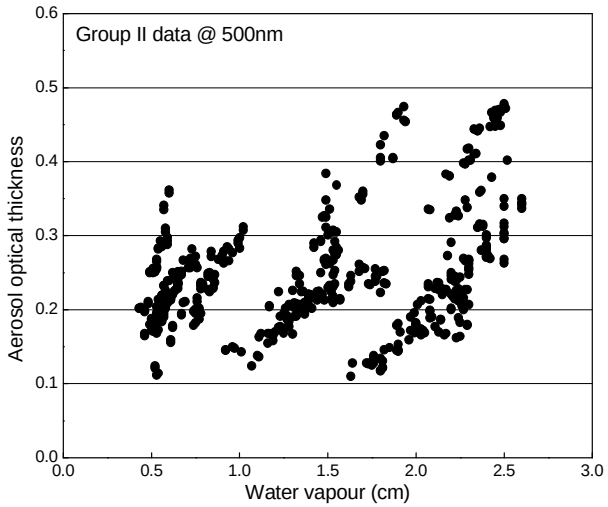

Fig. 8. Mass plot of AOT versus water vapour for Group II data sets at 500nm

observation during the three years. From Table 2 it is clear that the slopes vary largely. Further, it is observed that a correlation between the slope and the range of water vapour is difficult month-wise or by seasons or by years. In order to obviate this difficulty, a different method is followed.

A graphical plot of the slope versus month is shown in the Fig. 6. From Fig. 6, it can be seen that the data could be classified into Group I with slope ≤ 0.25 and Group II with slope > 0.25. AOT versus water vapour plot for the data coming under Group I is shown in Fig. 7. It can be seen from the figure that the AOT increases linearly with water vapour. By least squares fitting of the data, the average growth rate given by the slope is found to be 20%.

The data falling under group II are graphically presented in Fig. 8. This scatter diagram shows the data being distributed into three distinct groups. Each of the groups is characterized by a distinct range of water vapour and slope.

8.2. *Growth rate features of AOT at 1020 nm*

Following the procedure similar to that of 500nm, the data could be classified into Group I with slope ≤ 0.12 and Group II with slope > 0.12. Treating the two groups as in the case of 500nm, the growth rates are obtained. The results are shown in Table 3.

9. Discussion

The present study shows that the AOT does not increase continuously with the water vapour of the

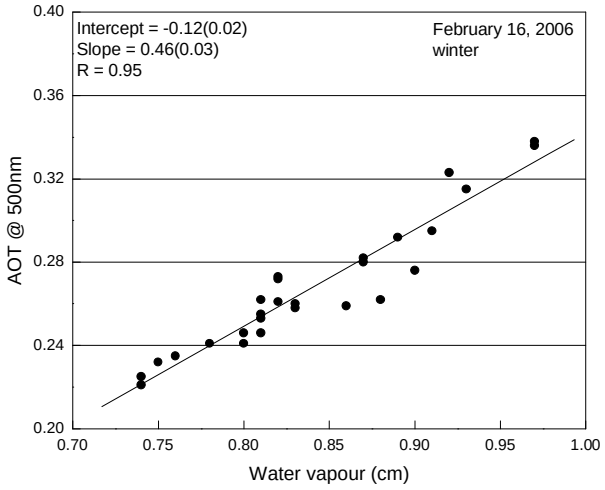

Fig. 9. Growth rate features of AOT and water vapour for a particular day in winter

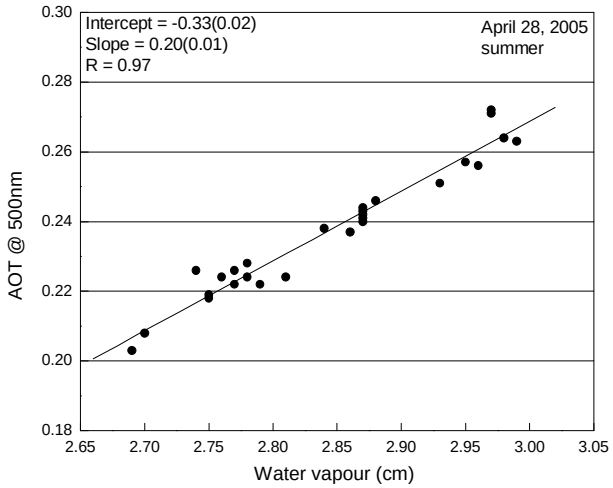

Fig. 10. Growth rate features of AOT and water vapour for a particular day in summer

atmosphere. From the Figs. 9 & 10 it is clear that the growth rate at shorter wavelength is higher than at longer wavelength. Though the summer (March-May) water vapour content is high compared to winter (December-February) water vapour, the growth rate is high in winter. Since the temperature is high during the summer, the evaporation rate of water is high and the growth of AOT decreases at faster rate.

The growth rates of AOT with the ranges of water vapour could be explained in the following way. Starting with the lowest value of water vapour, the AOT grows to a maximum value at certain value of water vapour which indicates the maximum water vapour that aerosol can hold. At this stage, there will be a gravitational settling giving rise to a decreased density of aerosols. It results in the reduced value of AOT.

TABLE 3

Slope values for the mass-plot of AOT versus water vapour [@ 1020nm] for different months during three years

Month	Slope	Range of water vapour in cm (min – max)
December 2003	0.13	0.54-1.12
January 2004	0.08	0.57-1.29
February 2004	0.13	0.56-0.90
	0.14	0.84-0.98
March 2004	0.12	0.53-1.28
April 2004	0.06	1.54-2.47
December 2004	0.12	0.42-1.29
	0.05	1.24-1.81
January 2005	0.27	0.43-0.6
	0.17	0.77-1.05
	0.10	1.40-1.74
February 2005	0.23	0.46-0.83
	0.14	0.85-1.46
March 2005	0.12	0.79-1.52
	0.21	0.73-1.03
November 2005	0.13	1.12-1.56
	0.14	1.56-1.81
December 2005	0.12	0.45-0.89
	0.25	0.99-1.48
	0.13	1.59-2.09
January 2006	0.15	0.49-1.43
	0.09	1.54-2.51
February 2006	0.25	0.44-1.07
	0.20	0.81-1.36
	0.18	1.11-1.55
	0.37	1.70-1.93
March 2006	0.09	1.10-2.00
	0.10	2.20-2.60
April 2006	0.07	1.57-2.25
	0.31	2.22-2.39
May 2006	0.32	2.07-2.38
	0.19	2.29-2.51
June 2006	0.14	2.37-2.48

Further increase in water vapour gives rise to the particle growth and increased AOT until another gravitational settling takes place. The repetition of this process results in the increase and decrease of AOT. The study clearly indicates that the increase in the water vapour content of the atmosphere need not continuously enhance the AOT. Therefore, the growth of AOT is a combined effect of the water vapour content and the temperature to a larger extent with other meteorological factors to some extent. This is in contrast to the observations made by the others according to which the AOT increases with the increase of water vapour (Smirnov *et al.*, 2002 ; Satheesh *et al*., 1999).

10. Conclusion

Dependence of spectral AOT on atmospheric water vapour has been analysed. The results are presented typically for two wavelengths, one at 500 nm and the other at 1020 nm. The data covers the period from December 2003 to June 2006. Growth rate of AOT is found to be larger at shorter wavelength (500 nm) than that of longer wavelength (1020 nm). For any single month, a mass-plot representation is followed. It is a graphical plot of AOT versus water vapour for a single wavelength of the scans for all the clear sky days of a particular month. The mass-plots showed a linear variation of AOT with water vapour. Of the two trends observed, one gave a larger slope for low water vapour content, whereas the other one gave a smaller slope when the water vapour content is high. Though the summer water vapour content is high compared to winter water vapour, the growth rate is high in winter. Since the temperature is high during the summer, the evaporation rate of water is high and the growth of AOT decreases at faster rate. Therefore, the growth of AOT is a combined effect of the water vapour content and the temperature to a larger extent with other meteorological factors to some extent.

Acknowledgement

The authors thank the Indian Space Research Organization for the financial assistance through the RESPOND scheme. The University of Mysore is thanked for the facilities. Special thanks to Late Prof. B. Narasimhamurthy for his kind support. My sincere thanks to the Management of PESIT and to my colleagues in the department for their constant encouragement.

References

Cachorro, V. E., deFrutos, A. M. and Casanova, J. L., 1987, "Determination of the Angstrom turbidity parameters", *Appl. Opt*., **26**, 3069-3081.

Eck, T. F., Holben, B. N., Dubovik, O., Smirnov, A., Slutsker, I., Lobert, J. M. and Ramanathan, V., 2001, "Column integrated aerosol optical properties over the Maldives during the N.E monsoon for 1998-2000", *Journal of Geophysical Research*, **106 (D22)**, 28555-28566.

Faizoun, C. A., Podaire, A. and Dedieu, G., 1994, "Monitoring of Sahelian Aerosol and Atmospheric water vapour content characteristics from Sun Photometer measurement", *Journal of applied meteorology*, **33**, 1291-1304.

Ganesh, K. E., Umesh, T. K. and Narasimhamurthy, B., 2009, "Aerosol Optical Thickness Measurements on Tsunami Day at a Continental Station", *Mysore. Aerosol and Air Quality Research*, **9**, 1, 94-104.

Iqbal, M., 1983, "An introduction to solar radiation", Academic Press, Ontario, Canada, 90-93.

Jacob, D., 2001, "The Role of Water Vapour in the Atmosphere: A Short Overview from a Climate Modeller's Point of View", *Phys. Chem. Earth (A)*, **26**, 523-527.

Kaufman, Y. J., Gitelson, A., Karnieli, A., Ganor, E., Fraser, Rs., Nakajima, T., Mattoo, S. and Holben, B. N., 1994, "Size distribution and scattering phase function of aerosol particles retrieved from sky brightness measurements", *J. Geophys. Res*., **99**, 10341-10351.

McCartney, E. J., 1976, "Optics of the Atmosphere", John Wiley, New York, NY, 114-126.

Narasimhamurthy, B., Raju, N. V., Thukarama, M., Prasad, B. S. N. and Krishnamoorthy, K., 1998, "MWR studies of the temporal and spectral features of atmospheric aerosols over Mysore (12.3° N): Global change studies", ISRO-GBP: GCS-02-98, 1998 (Indian Space Research Organization, Bangalore), page 77.

Prabha Nair, R., Krishna Moorthy, K., 1998, "Effects of changes in atmospheric water vapour content on physical properties of atmospheric aerosols at a coastal station", *Journal of Atmospheric and Solar-Terrestrial Physics*, **60**, p563.

Satheesh, S. K., Ramanathan, V., Li-Jones, X., Lobert Podgorny, J. M., Prospero, J. M., Holben, B. N. and Loeb, N. G., 1999, "A model for the natural and anthropogenic aerosols over the tropical Indian Ocean derived from Indian Ocean Experiment data", *J. Geophys. Res*., **27**, p421.

Smirnov, A., Holben, B. N., Dubovik, O., O'Neill, N. T., Eck, T. F., Westphal, D. L., Goroch, A. K., Pietras, C. and Slutsker, I., 2002, "Atmospheric aerosol optical properties in Persian Gulf", *Journal of Atmospheric Science*, **59**, 620-634.

Solar light company, 2002, Document No. Mtp06. USA, 5-50.

Suresh, T. and Elgar, Desa, 2005, "Seasonal variation of aerosol over Dona Paula, a coastal site on the west coast of India", *Journal of Atmospheric Environment*, **39**, 3471-3480.

Twomey, 1977, "The Influence of Pollution on the Shortwave Albedo of Clouds", *Journal of the Atmospheric Sciences*, **34**, 1149-1152.